A study of the ^{16}O(e,e′p) reaction at deep missing energies

N. Liyanage,[17] B. D. Anderson,[13] K. A. Aniol,[2] L. Auerbach,[29] F. T. Baker,[7] E. J. Beise,[16] J. Berthot,[1] W. Bertozzi,[17] P. -Y. Bertin,[1] L. Bimbot,[22] W. U. Boeglin,[5] E. J. Brash,[24] V. Breton,1 H. Breuer,[16] E. Burtin,[26] J. R. Calarco,[18] L. Cardman,[30] G. D. Cates,[23] C. Cavata,[26] C. C. Chang,[16] N. S. Chant,[16] J. -P. Chen,[30] E. Cisbani,[12] D. S. Dale,[14] A. Deur,[1] B. Diederich,[21] P. Djawotho,[33] B. Doyle,[14] J. -E. Ducret,[26] M. B. Epstein,[2] L. A. Ewell,[16] J. M. Finn,[33] K. G. Fissum,[17] H. Fonvieille,[1] B. Frois,[26] S. Frullani,[12] J. Gao,[17] F. Garibaldi,[12] A. Gasparian,[8,14] S. Gilad,[17] R. Gilman,[25] A. Glamazdin,[15] C. Glashausser,[25] J. Gomez,[30] V. Gorbenko,[15] T. Gorringe,[14] K. Griffieon,[33] F. W. Hersman,[18] R. Holmes,[28] M. Holtrop,[18] N. d'Hose,[26] C. Howell,[4] G. M. Huber,[24] C. E. Hyde-Wright,[21] M. Iodice,[12] C. W. de Jager,[30] S. Jaminion,[1] M. K. Jones,[33] K. Joo,[32] C. Jutier,[1,21] W. Kahl,[28] S. Kato,[34] J. J. Kelly,[16] S. Kerhoas,[26] M. Khandaker,[19] M. Khayat,[13] K. Kino,[31] W. Korsch,[14] L. Kramer,[5] K. S. Kumar,[23] G. Kumbartzki,[25] G. Laveissière,[1] R. De Leo,[10] A. Leone,[11] J. J. LeRose,[30] L. Levchuk,[15] M. Liang,[30] R. A. Lindgren,[32] G. J. Lolos,[24] R. W. Lourie,[27] R. Madey,[8,13,30] K. Maeda,[31] S. Malov,[25] D. M. Manley,[13] P. Markowitz,[5] D. J. Margaziotis[2] J. Marroncle,[26] J. Martino,[26] J. S. McCarthy,[32] K. McCormick,[21] J. McIntyre,[25] R. L. J. van der Meer,[24] Z. -E. Meziani,[29] R. Michaels,[30] J. Mougey,[3] S. Nanda,[30] D. Neyret,[26] E. A. J. M. Offermann,[30] Z. Papandreou,[24] C. F. Perdrisat,[33] R. Perrino,[11] G. G. Petratos,[13] S. Platchkov,[26] R. Pomatsalyuk,[15] D. L. Prout,[13] V. A. Punjabi,[19] T. Pussieux,[26] G. Quéméner,[33] R. D. Ransome,[25] O. Ravel,[1] Y. Roblin[1] R. Roché,[6] O. A. Rondon-Aramayo,[32] P. G. Roos,[16] D. Rowntree,[17] G. Rutledge,[33] P. M. Rutt,[25] A. Saha,[30] T. Saito,[31] A. J. Sarty,[6] A. Serdarevic-Offermann,[24] T. P. Smith,[18] A. Soldi,[20] P. Sorokin,[15] P. Souder,[28] R. Suleiman,[13] J. A. Templon,[7] T. Terasawa,[31] L. Todor,[21] H. Tsubota,[31] H. Ueno,[34] P. E. Ulmer,[21] G. Urciuoli,[12] P. Vernin,[26] S. van Verst,[17] B. Vlahovic,[20] H. Voskanyan,[35] J. W. Watson,[13] L. B. Weinstein,[21] K. Wijesooriya,[33] R. Wilson,[9] B. Wojtsekhowski,[30] D. G. Zainea,[24] V. Zeps,[14] J. Zhao,[17] Z. -L. Zhou,[17]

(The Jefferson Lab Hall A Collaboration)

[1] *Université Blaise Pascal/IN2P3, F-63177 Aubière, France*
[2] *California State University, Los Angeles, California, 90032*
[3] *Institut des Sciences Nucléaires, F-38026 Grenoble, France*
[4] *Duke University, Durham, North Carolina, 27706*
[5] *Florida International University, Miami, Florida, 33199*
[6] *Florida State University, Tallahassee, Florida, 32306*
[7] *University of Georgia, Athens, Georgia, 30602*
[8] *Hampton University, Hampton, Virginia 23668*
[9] *Harvard University, Cambridge, Massachusetts, 02138*
[10] *INFN, Sezione di Bari and University of Bari, I-70126 Bari, Italy*
[11] *INFN, Sezione di Lecce, I-73100 Lecce, Italy*
[12] *INFN, Sezione Sanitá and Istituto Superiore di Sanitá, Laboratorio di Fisica, I-00161 Rome, Italy*
[13] *Kent State University, Kent, Ohio, 44242*
[14] *University of Kentucky, Lexington, Kentucky, 40506*
[15] *Kharkov Institute of Physics and Technology, Kharkov 310108, Ukraine*
[16] *University of Maryland, College Park, Maryland, 20742*
[17] *Massachusetts Institute of Technology, Cambridge, Massachusetts, 02139*
[18] *University of New Hampshire, Durham, New Hampshire, 03824*
[19] *Norfolk State University, Norfolk, Virginia, 23504*
[20] *North Carolina Central University, Durham, North Carolina, 27707*
[21] *Old Dominion University, Norfolk, Virginia, 23508*
[22] *Institut de Physique Nucléaire, F-91406 Orsay, France*
[23] *Princeton University, Princeton, New Jersey, 08544*
[24] *University of Regina, Regina, Saskatchewan, Canada, S4S 0A2*
[25] *Rutgers, The State University of New Jersey, Piscataway, New Jersey, 08854*
[26] *CEA Saclay, F-91191 Gif-sur-Yvette, France*
[27] *State University of New York at Stony Brook, Stony Brook, New York, 11794*
[28] *Syracuse University, Syracuse, New York, 13244*
[29] *Temple University, Philadelphia, Pennsylvania, 19122*
[30] *Thomas Jefferson National Accelerator Facilty, Newport News, Virginia, 23606*
[31] *Tohoku University, Sendai 980, Japan*
[32] *University of Virginia, Charlottesville, Virginia, 22901*
[33] *College of William and Mary, Williamsburg, Virginia, 23187*
[34] *Yamagata University, Yamagata 990, Japan*

[35] *Yerevan Physics Institute, Yerevan 375036, Armenia*
(April 30, 1999)

The ^{16}O(e,e'p) reaction was studied in the quasielastic region at $q = 1000$ MeV and $\omega = 445$ MeV. R_L, R_T and R_{LT} response functions were extracted for $25 < E_{miss} < 60$ MeV and $P_{miss} < 280$ MeV/c.

for $p_{miss} < 150$ MeV/c, R_L and R_T are mostly accounted for by the DWIA and HF models of s-shell knockout for $E_{miss} < 50$ MeV. For $E_{miss} > 50$ MeV , R_T remains strong while R_L appears to go to zero. At $p_{miss} \approx 280$ MeV/c, R_L is consistent with zero and with theory. R_T and R_{LT} are much bigger than the DWIA calculation but the same size as the HF calculation.

The coincidence (e,e′p) reaction in quasielastic kinematics ($\omega = Q^2/2m_p$ where q_μ and ω are the four-momentum and energy transfers) has long been a crucial tool in the study of nuclear structure. (e,e′p) cross section measurements have provided both a wealth of information on the wave functions of protons inside the nucleus and stringent tests of nuclear theories. Response function measurements have provided detailed information about the different reaction channels contributing to the cross section such as single- and multi-nucleon knockout, meson exchange currents, isobar excitations, and final state interactions.

Originally, the quasielastic cross section was attributed entirely to single particle knockout from the valence states of the nucleus. However, a series of ^{12}C(e,e′p) experiments performed at MIT-Bates [1], [2], [3], [4] which sampled various kinematic regions measured much larger cross sections at high missing energy ($E_{miss} = \omega - T_p$ where T_p is the final proton kinetic energy) than was expected for single particle knockout. Separated C(e,e′p) coincidence data reported by Ulmer *et al* [1] show a dramatic increase in the transverse-to-longitudinal ratio above the two-particle emission threshold. This enhancement indicates the presence of an additional, transverse, non-quasielastic reaction mechanism. The longitudinal response becomes consistent with zero above $E_{miss} = 50$ MeV, indicating that single particle knockout is very small above this point. Similar R_T/R_L enhancement has been observed at NIKHEF-K for ^{6}Li [5] and ^{12}C [6]. These findings indicate that a large part of the cross section at large missing energies comes from two-body and multi-body processes.

There have been several theoretical attempts to explain the continuum strength using many-body knockout models, but no model can explain all the data [7], [8], [9]. It has also been suggested that short-range and tensor correlations could play a major role in populating the high E_{miss} continuum. Muther *et al.* [10] calculated the effects of these correlations in ^{16}O and have shown that they shift strength from conventional quasi-hole states to high-E_{miss}, high-P_{miss} channels.

In this experiment we measured the ^{16}O(e,e′p) reaction in the quasielastic region at $|\vec{q}| = 1000$ MeV and $\omega = 445$ MeV. We extracted the longitudinal (R_L), transverse (R_T) and longitudinal-transverse (R_{LT}) response functions from cross sections measured at several beam energies (E_0) and electron angles (θ_e) for $E_{miss} < 60$ MeV and $P_{miss} < 280$ MeV/c. This was the first Jefferson Lab Hall A experiment and the first response function separation on a complex nucleus at large (P_{miss}, E_{miss}). This paper reports the results for $E_{miss} > 25$ MeV.

We scattered the continuous incident electron beam from a waterfall target [11] and detected the scattered electrons in the High Resolution Electron Spectrometer (HRS$_e$) and the protons in the High Resolution Hadron Spectrometer (HRS$_h$) [12]. The HRS$_e$ detector package consisted of two scintillator planes to generate the trigger, a gas Cherenkov detector for particle identification and a pair of two-plane Vertical Drift Chambers (VDCs) for trajectory determination. On HRS$_h$ only the VDCs and trigger scintillators were used for this experiment.

The waterfall target consisted of three flat flowing water 'foils', each approximately 130 mg/cm^2 thick along the beam and at 30° to the incident beam. Using three foils improved our target energy loss determination and allowed us to use vertex cuts to reject accidentals.

We measured the ^{16}O(e,e′p) cross-sections at three beam energies, 0.843, 1.643 and 2.442 GeV, keeping $|\vec{q}|$ and ω fixed, in order to vary the virtual photon polarization. At 2.442 GeV, we measured the cross section for six different proton-virtual photon angles, $\theta_{pq} = 0°, \pm 8°, \pm 16°$, and $\pm 20°$. At 0.843 GeV, we measured at $\theta_{pq} = 0°, +8°$, and $+16°$. $\theta_{pq} = 0°$ and $\pm 8°$ measurements at 1.643 GeV provided redundancy for checking systematic uncertainties. These measurements allowed us to separate R_L and R_T at $\theta_{pq} = 0°$ and $R_L + \frac{V_{TT}}{V_L} R_{TT}, R_T$ and R_{LT} at $\theta_{pq} = 8°$ and 16°.

The accuracy of a response function separation depends on matching the values of $|\vec{q}|$ and ω between different kinematic settings with different virtual photon polarizations. In order to match $|\vec{q}|$ and locate $\vec{q}$, we measured H(e,e′p) (also present in the waterfall target) with a pin-hole collimator on HRS$_e$. The momentum of the detected protons is equal to $\vec{q}$. We determined the location of the H(e,e′p) momentum peak to $\frac{\delta p}{p} = 2 \times 10^{-4}$ allowing us to match $|\vec{q}|$ to 2×10^{-4} between different kinematic settings. Throughout the experiment H(e,e′) data, measured simultaneously with the ^{16}O(e,e′p) data, provided a continuous monitor of luminosity and beam energy.

In the first Born approximation the non-polarized (e,e′p) cross section can be expressed as [13]

$$\frac{d^6\sigma}{d\Omega_e d\Omega_p d\omega dE_{p'}} = \frac{p' E_{p'}}{(2\pi)^3} \sigma_{Mott} (V_L R_L + V_T R_T + V_{LT} R_{LT} \cos\phi + V_{TT} R_{TT} \cos 2\phi), \quad (1)$$

where V_L, V_T, V_{LT} and V_{TT} are kinematic factors dependent upon the electron vertex, ϕ is the angle between the electron scattering plane and the reaction plane, and σ_{Mott} is the Mott cross section.

In parallel kinematics, because the out-of-plane angle ϕ is not defined only $R_{\rm L}$ and $R_{\rm T}$ survive in the expression for the cross section. The Rosenbluth method may be used to separate R_L and R_T. In the case of perpendicular kinematics, all four terms are present in the expression for the cross section. By measuring the cross section on both sides of $\vec{q}$ ($\phi = 0°$ and $\phi = 180°$) keeping all other kinematic variables constant, $R_{\rm LT}$ can be extracted according to

$$R_{LT} = \frac{(2\pi)^3}{E'_p p'_p \sigma_{Mott}} \left[\frac{\sigma(0°) - \sigma(180°)}{2V_{LT}} \right] \quad (2)$$

The separation of $R_{\rm TT}$ requires an out-of-plane measurement. An in-plane Rosenbluth separation in the case of perpendicular kinematics allows for the separation of $R_L + \frac{V_{TT}}{V_L} R_{TT}$ and R_T.

For the "parallel" kinematic setting of this experiment ($\theta_{pq} = 0°$) the H(e,e'p) peak and the associated radiative tail were present in the coincidence phase-space for ^{16}O. To remove H(e,e'p) events we cut out all events with $P_{miss} < 45$ MeV/c. This cut significantly reduced the ^{16}O(e,e'p) statistics for this setting. This cut removed a large fraction of the events with $\vec{P}_{miss} \parallel \vec{q}$. However, since the remaining events have $\vec{P}_{miss}$ symmetrically distributed around $\vec{q}$, this data sample is approximately parallel, in that the interference response functions, which are dependent on ϕ (the azimuthal angle around $\vec{q}$), average out to zero. Due to this problem we call this setting "quasi-parallel" kinematics. The perpendicular kinematic settings had no contamination due to H.

Figs. 1- 3 present the separated response functions from this experiment for $|\theta_{pq}| = 0, 8°$ and 16° corresponding to missing momenta of approximately 60, 145 and 280 MeV/c. Note that 280 MeV/c is larger than the fermi momentum of oxygen, $p_F \approx 220$ MeV/c.

To check how much of the observed continuum strength can be explained by $1s_{1/2}$ knockout, we compared our results to $1s_{1/2}$ single particle knockout calculations by Van Orden [14], [15], Kelly [13] and Ryckebusch [16], [17], [18]. The Ryckebusch calculations (Impulse Approximation (IA) calculations and calculations that include two-body current contributions related to Meson Exchange Currents (MECs and Δ-creation) have been performed in a self-consistent Hartree-Fock (HF) frame work. Kelly calculations are non-relativistic DWIA (Distorted Wave Impulse Approximation) calculations while Van Orden calculations are relativistic DWIA.

We distributed the calculated $1s_{1/2}$ response functions in E_{miss} using a prescription given by Jeukenne and Mahaux [19], [7], where the $1s_{1/2}$ profile is modeled using a Lorentzian with an energy-dependent width $\Gamma(E)$. This shape described the $p_{miss} \approx 60$ MeV/c data well (see Fig.1) but did not describe the higher p_{miss} data well.

Fig. 1 presents the separated response functions for the "quasi-parallel" kinematic setting. The wide bump centered around $E_{miss} = 40$ MeV in both R_L and R_T corresponds primarily to single particle knockout from the $1s_{1/2}$ state. The difference between the transverse and longitudinal spectral functions ($S_T - S_L$), which is expected to be zero for a free nucleon, is nonzero for $E_{miss} > 40$ MeV. This is in qualitative agreement with the high E_{miss} behavior of R_L and R_T observed at MIT-Bates by Ulmer *et al.* [1]. However, the errors on $S_T - S_L$ are too large to draw any conclusions about the onset of the difference.

Fig. 2 presents the separated response functions for the $|\theta_{pq}| = 8°$ perpendicular kinematic setting, ($p_{miss} \approx 145$ MeV/c). At this point R_T is approximately constant for the entire range of missing energy measured ($25 < E_{miss} < 60$ MeV) whereas $R_L + V_{TT}R_{TT}/V_L$ becomes consistent with zero for $E_{miss} > 50$ MeV. Since $\frac{V_{TT}}{V_L} R_{TT}$ is estimated to be about 7% of R_L, this behavior can be attributed mainly to R_L. R_{LT} peaks at about 40 MeV but is always negative, indicating that R_L is not zero. R_{LT} is about one-third the size of R_T. The Mahaux parameterization does not reproduce the missing energy shape of R_L or R_T.

All four calculations underestimate the measured R_{LT} over the whole range of E_{miss}. As in the case of quasi-parallel kinematics, the inclusion of MEC+Δ in the HF calculation seems to bring it closer to the data (and to the relativistic DWIA calculation). For $E_{miss} < 35$ MeV, all response functions are larger than the calculations. For $E_{miss} > 50$ MeV, $R_L + \frac{V_{TT}}{V_L} R_{TT}$ is consistent with both zero and the calculations. R_T, on the other hand, appears to retain strength above 50 MeV. This is in agreement with the parallel kinematics results of the present experiment and also with the results reported by Ulmer *et al.* [1].

Fig. 3 presents the separated response functions for the $|\theta_{pq}| = 16°$ perpendicular kinematic setting, $p_{miss} \approx 280$ MeV/c. At this point, R_T and R_{LT} appear to slowly decrease over $25 < E_{miss} < 60$ MeV whereas $R_L + V_{TT}R_{TT}/V_L$ is consistent with zero. R_{LT} is about one-third the size of R_T. The shapes of R_T and R_{LT} are not consistent with Mahaux's parameterization.

At $p_{miss} \approx 280$ MeV/c, the total HF calculation predicts much higher strength for all the response functions than the DWIA calculations. R_L is close to zero as expected by all three calculations. However, R_T and R_{LT} are much larger than the DWIA calculation and approximately as large as the HF-RPA calculation. Neither R_T nor R_{LT} show a peak at $E_{miss} \approx 40$ MeV corresponding to single particle knockout from the s-shell.

Fig. 4 shows the cross sections measured over the whole range of missing momenta covered by this experiment. The cross sections are compared to $1s_{1/2}$ single particle knockout calculations by Van Orden [14], [15] folded in with the energy dependent Lorentzian parameterization by Mahaux. At $< P_{miss} >= 50$ MeV, the Lorentzian shape exactly explains the measured cross section. We determined the spectroscopic factor used with all Van Orden calculations presented here by fitting to this data. For the $1s_{1/2}$-shell the spectroscopic factor thus determined was 0.88. Note that this is significantly higher than the previously reported spectroscopic factors for the $1s_{1/2}$-shell [20].

As P_{miss} increases, the single particle knockout calculation accounts for only a fraction of the measured strength. Furthermore, for the two settings with P_{miss} above the Fermi momentum, the measured cross section profiles do not exhibit any resemblance to the expected $1s_{1/2}$ Lorentzian shape. This clearly indicates that the

cross section measured at high P_{miss} and high E_{miss} is mostly of non-single particle origin.

In summary, for $45 < p_{miss} < 75$ MeV/c, R_L and R_T are close to DWIA and HF-RPA models of s-shell knockout. The difference between the transverse and longitudinal spectral functions ($S_T - S_L$), which is expected to be zero for a free nucleon, is nonzero for $E_{miss} > 40$ MeV and is about half the size of the spectral function difference measured on carbon at $q = 400$ MeV/c [1]. This might indicate that the non-single particle knockout mechanisms responsible for the $L-T$ difference decrease faster with q than the nucleon form factors. At $p_{miss} \sim 150$ MeV/c R_L and R_T are mostly accounted for by the DWIA and HF-RPA models of s-shell knockout for $E_{miss} < 50$ MeV. For $E_{miss} > 50$ MeV, R_T remains strong while R_L appears to go to zero. At $p_{miss} \approx 280$ MeV/c R_L is consistent with zero and with theory. R_T and R_{LT} are significantly bigger than the DWIA prediction but are comparable to the HF-RPA calculations.

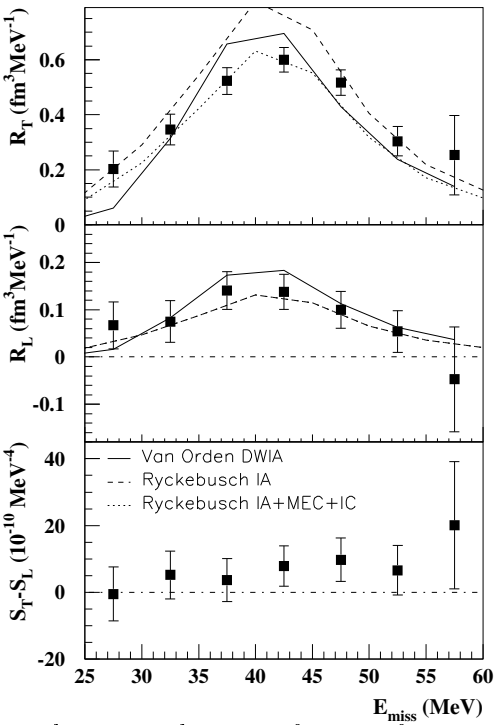

FIG. 1. The separated response functions for quasi-parallel kinematics for 45 MeV/c $< p_{miss} <$ 75 MeV/c.

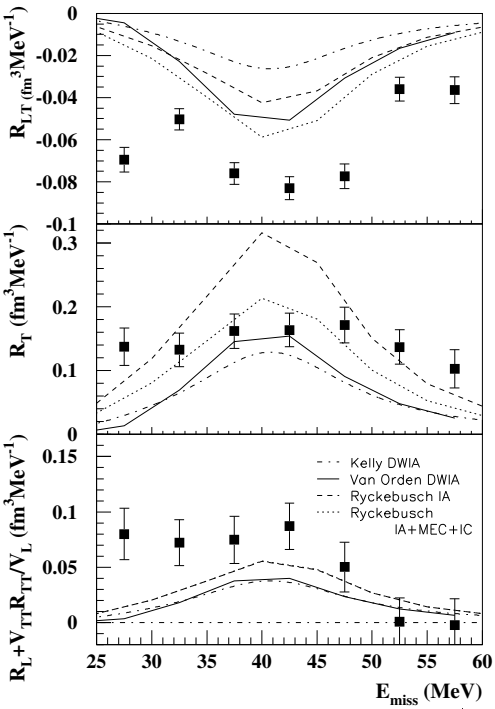

FIG. 2. Separated response functions for the $|\theta_{pq}| = 8°$ setting ($P_{miss}^{average} \approx 145$ MeV/c). Plots show (from top to bottom) R_{LT}, R_T, and $R_L + \frac{V_{TT}}{V_L} R_{TT}$.

[1] P.E. Ulmer *et al.,* Phys. Rev. Lett. **59,** 2259 (1987).
[2] R. Lourie *et al.,* Phys. Rev. Lett. **56,** 2364 (1986).
[3] L. Weinstein *et al.,* Phys. Rev. Lett. **64,** 1646 (1990).
[4] J.H. Morrison, Ph.D. thesis, MIT (1993).
[5] J.B.J.M. Lanen *et al.,* Phys. Rev. Lett. **64,** 2250 (1990).
[6] G. van der Steenhoven *et al.,* Nucl. Phys. **A480,** 547 (1988).
[7] J. Ryckebusch *et al.,* Nucl. Phys. **A624,** 581 (1997).
[8] A. Gil *et al.,* Nucl. Phys. **A627,** 599 (1997).
[9] T. Takaki, Phys. Rev. C **39,** 359 (1989).
[10] H. Muther and W.H. Dickhoff *et al.,* Phys. Rev. C **49,** R17 (1994).
[11] F. Garibaldi *et al.,* Nucl. Instrum. Methods **A314,** 1 (1992).
[12] N. Liyanage, Ph.D. thesis, MIT (1999).
[13] J.J. Kelly, Adv. Nucl. Phys., **23** ed. by J.W. Negele and E. Vogt 75 (1996).
[14] A. Picklesimer, J. W. Van Orden, and S. J. Wallace, Phys. Rev. C **32**, 1312 (1985).
[15] A. Picklesimer and J. W. Van Orden, Phys. Rev. C **40**, 290 (1989).
[16] J. Ryckebusch *et al.,* Nucl. Phys. **A476,** 237 (1988).
[17] J. Ryckebusch *et al.,* Nucl. Phys. **A503,** 694 (1989).
[18] V. Van der Sluys, K. Heyde, J. Ryckebusch, M. Waroquier, Phys.Rev. C **55** (1997) 1982
[19] J.P. Jeukenne and C. Mahaux, Nucl. Phys. **A394,** 445 (1983).
[20] W. Bertozzi, Nucl. Phys. **A527,** 347 (1991).

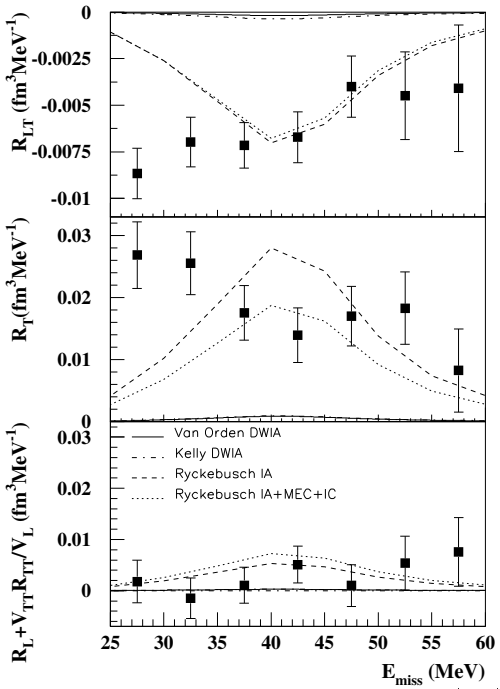

FIG. 3. Separated response functions for the $|\theta_{pq}| = 16°$ setting ($P_{miss}^{average} \approx 280.0$ MeV/c). Plots show (from top to bottom) R_{LT}, R_T, and $R_L + \frac{V_{TT}}{V_L} R_{TT}$.

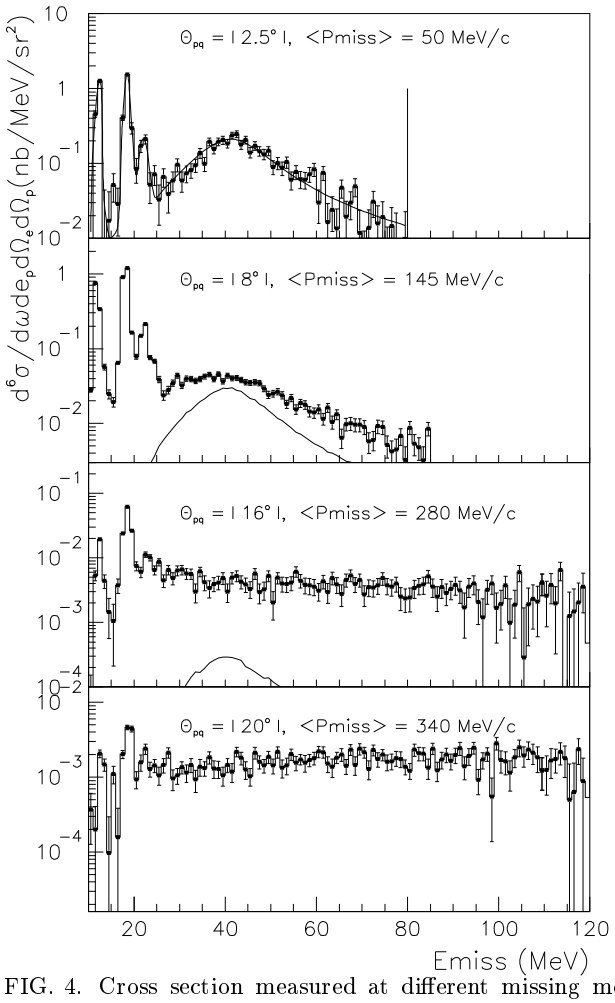

FIG. 4. Cross section measured at different missing momenta as a function of missing energy. The solid lines show the $1s_{1/2}$ single particle strength calculated by VanOrden folded in with the energy dependent Lorentzian parameterization by Mahaux. The s-shell spectroscopic factor used with the calculation was determined by fitting to the $\theta_{pq} = 2.5°$ data (top plot)